Journal of Operation and Automation in Power Engineering

Vol. 5, No. 1, June 2017, Pages: 75-82

http://joape.uma.ac.ir/

A Soft Switched DC-DC Boost Converter for Use in Grid Connected Inverters

*M. Pakdel, S. Jalilzadeh**

Department of Electrical Engineering, University of Zanjan, Zanjan, Iran

Abstract- *This paper presents a soft-switching DC-DC boost converter, which can be utilized in renewable energy systems such as photovoltaic array, and wind turbine connections to infinite bus of a big power network, using grid connected inverters. In the proposed topology for the DC-DC boost converter, the main and the auxiliary power switches are turned on and turned off with zero voltage switching (ZVS) and zero current switching (ZCS), respectively. Furthermore, by applying soft-switching techniques to driving power switches, the power losses and stresses associated with commutation of power devices decrease significantly. The efficiency of the proposed soft-switched DC-DC converter at various output powers is compared with that of the traditional DC-DC converter and a few topologies proposed in recent literature. This comparison indicates that the proposed DC-DC boost converter is much more efficient around the rated power (1 kW). The power topology and the control strategy applied to the proposed soft-switched DC-DC boost converter, which is connected to a grid-tied inverter, are analyzed theoretically by simulation studies. Moreover, an experimental prototype is implemented to verify the theoretical analysis and the simulation studies.*

Keyword: Soft switching, DC-DC converter, Zero voltage switching (ZVS), Zero current switching (ZCS), Grid connected inverters, Renewable energy systems.

1. INTRODUCTION

Grid-connected inverters have been developing quickly for renewable energy power converter applications due to the limited availability of traditional energy resources such as oil and coal and even nuclear materials. Furthermore, owing to dramatic and fast growth of energy demands all over the world, the cost-effective and reasonable solution is to utilize renewable energy resources such as solar and wind energies in lieu of traditional nonrenewable energy resources. However, the produced output power of renewable energy resources is generally unregulated and discontinuous. DC-DC boost converters are usually applied in order to convert the unregulated and discontinuous output power of such renewable energy resources to a constant output power. Various grid-tied inverter topologies and control strategies have been proposed in the literature [1-10]. Soft-switching techniques are employed extensively to decline commutation losses of power switches [11-20]. The purpose of soft-switching converters is to reduce power-switching losses and electromagnetic interference (EMI) more than the traditional hard-switching inverters. Therefore, to increase power efficiency, grid-tied inverters are also designed to be disconnected rapidly from the power network when it goes down, known as islanding phenomenon. According to the IEEE standard 1547 [8], the time required for disconnection of distributed generation systems (DGs) must not exceed two seconds after power network blackout. The grid-tied inverters may either include high-frequency transformers and conventional low-frequency transformers, or lack a transformer (transformerless). Inverters with high-frequency transformers involve converting high frequency AC power to DC and then DC to AC power network voltage again [9]. Transformerless inverters have higher efficiency; however, due to the lack of isolation between DC and AC, the circuit parts can lead to the transmission of dangerous DC faults to the AC side circuits [10]. The sine PWM technique is applied to decrease the harmonics contents at the output voltage of grid-tied inverters. Most grid-tied inverters use maximum power point tracking technique on their DC sides to extract the maximum power from the unregulated and discontinuous renewable energy resource. This renewable energy resource is usually a boost DC-DC converter with controllable power switch gate signal duty cycle according to variable power supplied from the renewable energy resource in order to provide constant DC link voltage for grid-tied inverters [11]. Several soft switching DC to DC topologies have been proposed in many studies [22-24]. A few studies also report

Received: 04 Sep. 2016
Revised: 29 Oct. 2016
Accepted: 20 Nov. 2016
*Corresponding author:
Email: jalilzadeh@znu.ac.ir (S. Jalilzadeh)

disadvantages such as the power switch not turning off with soft switching [21]. The soft switching condition depends on the duty cycle applied in literature [24]. A magnetically coupled inductor is applied in a ZVZCS converter [22] which causes unwanted oscillations to occur in response to the nonlinear characteristics of coupled inductors. In another study [25], additional current stress was produced which caused power loss in the ZVZCS converter. In literatures [26-31], a magnetically coupled inductor has been used. The switches are turned on with zero voltage switching) ZVS) ; however, they are not turned off in zero current switching) ZCS). Moreover, due to the nonlinear characteristics of coupled inductors there will be unwanted oscillations and inductor current leakages in the converter. In study [30] on the other hand, the voltage stress across the main switch is very high during the resonance mode. Coupled inductor based converters with arbitrary spike in voltage gain by changing the turn's ratio is more attractive. Voltage spike on the switches is the main issue of these converters. Passive clamp [32], [33] or active clamp [34], [35] technique is used to decline the voltage spike on the switches. However, in these converters there is a high voltage stress on the output diode. Therefore, a snubber circuit or higher rated diodes should be applied.

This paper introduces a novel soft-switching DC-DC boost converter, which can be deployed in renewable energy systems such as photovoltaic array and wind turbine connections to infinite bus of a big power network, using grid-connected inverters. To overcome the deficiencies mentioned earlier in literatures, in the proposed topology and control strategy, the power losses associated with commutation of power devices diminish significantly by using soft-switching techniques for driving power switches. The power topology and control strategy for the proposed soft-switched grid-tied inverter are investigated theoretically through simulation studies and demonstrated experimentally via prototype circuit testing.

2. PROPOSED TOPOLOGY AND CONTROL STRATEGY

The circuit schematic in Fig. 1 depicts the power circuit topology of the proposed soft-switched DC-DC boost converter, which is connected to a grid-tied inverter. The proposed topology is a novel soft-switched resonant DC-DC boost converter in a series of connections with a traditional full-bridge PWM converter. The series-connected circuit topology is assumed to include mass conduction losses. However, by applying soft-switching techniques through power switches, the associated power losses would decline considerably. Furthermore, all of the methods employed in grid-tied inverters such as maximum power point tracking (MPPT), power network synchronization, and islanding detection algorithms can be utilized in the proposed soft-switched grid-tied inverter. In operation mode I, power switches S_1 and S_2 are off, and then inductor L_{in} current flows through capacitors C_{S1} and C_1. In this mode, the following equation can be written:

$$L_{in}\frac{di}{dt}+\frac{1}{C_{S1}}\int_{t_0}^{t_1} i\,dt+\frac{1}{C_1}\int_{t_0}^{t_1} i\,dt=V_{in} \tag{1}$$

In operation mode II, power switch S_2 is turned on with ZVS. In contrast, power switch S_1 is off. In this mode, capacitor C_1 is discharged through diode of S_1. Moreover, the following relation can be written:

$$\frac{1}{C_1}\int_{t_1}^{t_2} i\,dt+L_{in}\frac{di}{dt}=-V_{in} \tag{2}$$

In operation mode III, power switch S1 is turned on with ZVS, and capacitor C1 and C2 are charged. Furthermore, in grid half positive cycle, power switches S3 and S6 are turned on with ZVS. The following equation is valid among the circuit elements:

$$L_{in}\frac{di}{dt}+L_{1}\frac{di}{dt}=V_{in} \tag{3}$$

where, L1 is the primary inductance of high frequency transformer. In operation mode IV, power switch S2 is turned off with ZVS. In this mode, power switches S3 and S6 are also turned off, and freewheeling current flows through diode of power switches S3 and S4. Moreover, we have the following equation:

$$L_{in}\frac{di}{dt}+L_1\frac{di}{dt}+\frac{1}{C_{S2}}\int_{t_3}^{t_5} i_1\,dt=V_{in} \tag{4}$$

In operation mode V, the power switch S_2 is turned on with ZVS.

In addition, capacitors C_2 and C_1 are charged and discharged by the power switch S_1 diode respectively. The following equation is also satisfied:

$$L_{in}\frac{di}{dt}-\frac{1}{C_1}\int_{t_5}^{t_6} i\,dt=-V_{in} \tag{5}$$

In operation mode VI, power switch S_1 is turned off with ZCS, and capacitors C_2 and C_1 are charged and discharged, respectively. The following equations can be used:

$$L_{in}\frac{di_1}{dt}+\frac{1}{C_{S1}}\int_{t_6}^{t_7} i_1\,dt+L_1\frac{di}{dt}=V_{in} \tag{6}$$

$$\frac{1}{C_1}\int_{t_6}^{t_7} i_2\,dt+L_1\frac{di}{dt}=0 \tag{7}$$

$$i_1+i_2=i \tag{8}$$

In operation mode VII, the power switch S_2 is turned off with ZCS conditions. In addition, we have the following equation:

$$L_{in}\frac{di}{dt}+\frac{1}{C_{S1}}\int_{t_7}^{t_8} i\,dt+\frac{1}{C_1}\int_{t_{10}}^{t_8} i\,dt=V_{in} \tag{9}$$

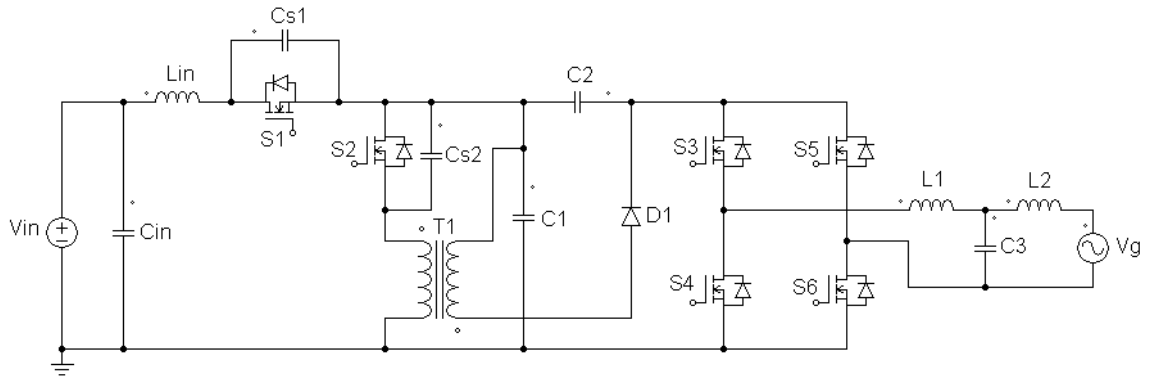

Fig. 1. Circuit schematic of the proposed soft-switched grid-tied inverter

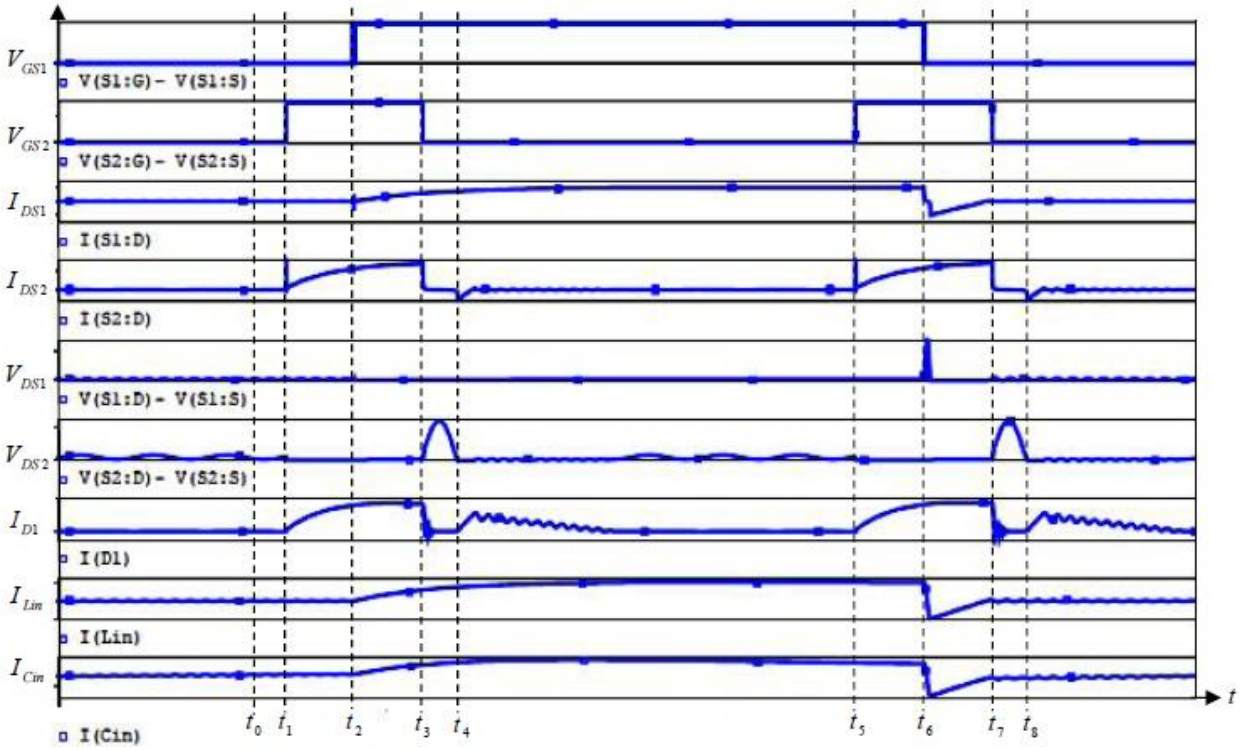

Fig. 2. Operation modes timing diagram for DC-DC converter section in the proposed soft switched grid tied inverter

Timing diagrams of various circuit parameters as well as soft-switching conditions for power switches S_1 and S_2 are depicted in Fig. 2.

The operation modes of the proposed grid-tied inverter topology are demonstrated in Fig. 3. For controlling the output power of the proposed grid-connected inverter, a current control method using alpha beta to dq transformation and vice versa (dq to alpha beta transformation) is applied. The block diagram of the applied current control strategy with output voltage phase locked loop (PLL) is shown in Fig. 4.

capacitor C_2 is its using adequate capacitance to reduce ripple current ratings. DC-link capacitor current is obtained by subtracting the input current from power MOSFET S_2 current (i_{DS2}). The frequency of DC-link capacitor C_2 current is approximately twice the switching frequency. Since there is an equivalent series resistance (R_S) in DC-link capacitor, thus the ripple voltage across capacitor C_2 can be written as follows:

$$\Delta V_{C2} = \frac{I_{in}}{C_2} D T_S \tag{10}$$

$$\Delta V_{RS} = i_{C2} \times R_S \tag{11}$$

$$\Delta V_{C2Eq} = \sqrt{\Delta V_{C2}{}^2 + \Delta V_{RS}{}^2} \tag{12}$$

where, I_{in}, D, and T_S are the drain current, duty cycle, and switching period of power switch S_1, respectively. Under specific output ripple voltage conditions, the value of capacitor C_2 can be estimated. As indicated in Fig. 2, the maximum drain current of power MOSFETs S_1, S_2, S_3, S_4, S_5, and S_6 as well as the maximum drain-to-source voltages across them in the proposed soft-switched grid-tied inverter are given as follows:

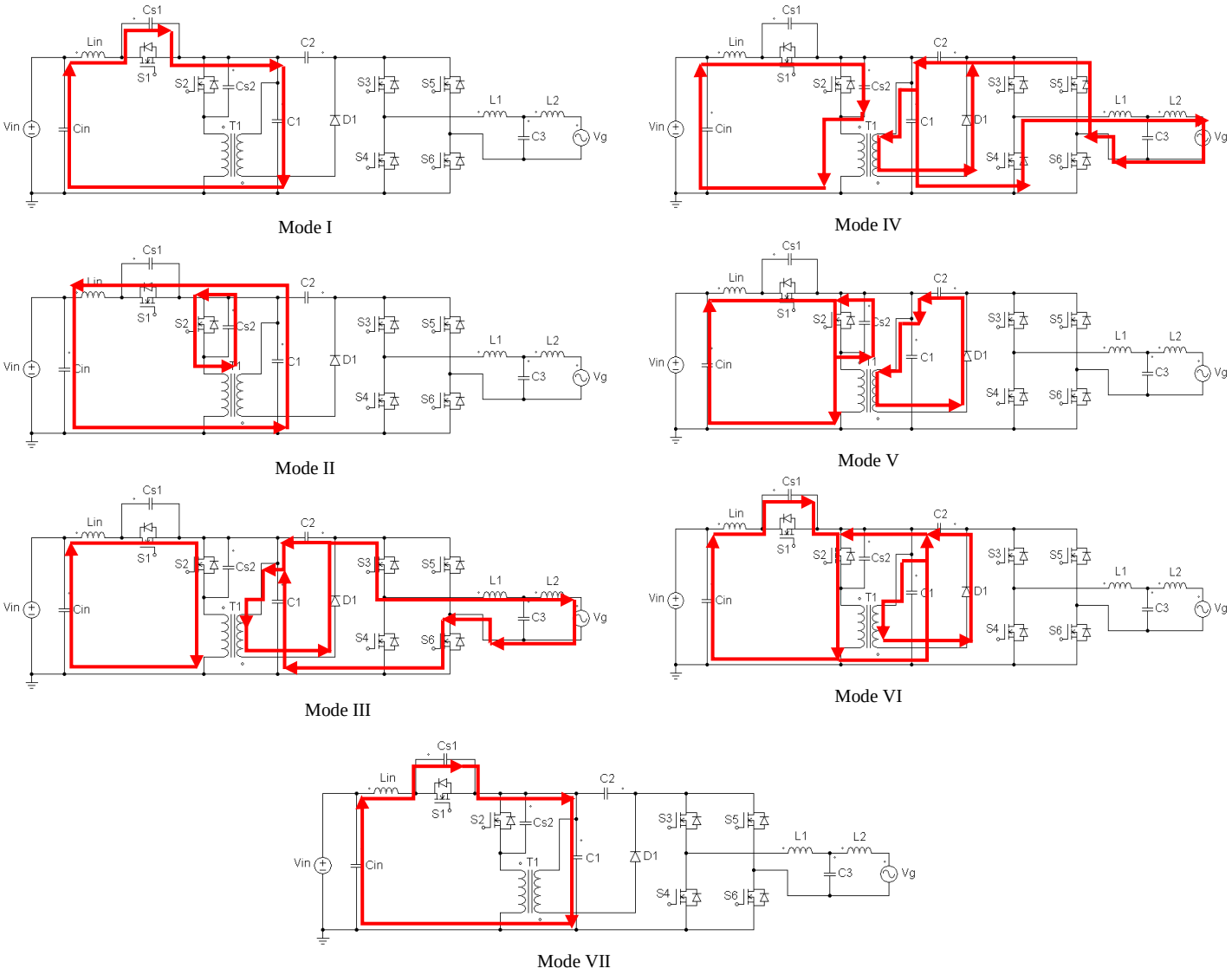

Fig. 3. Operation modes of proposed soft-switched grid-tied inverter

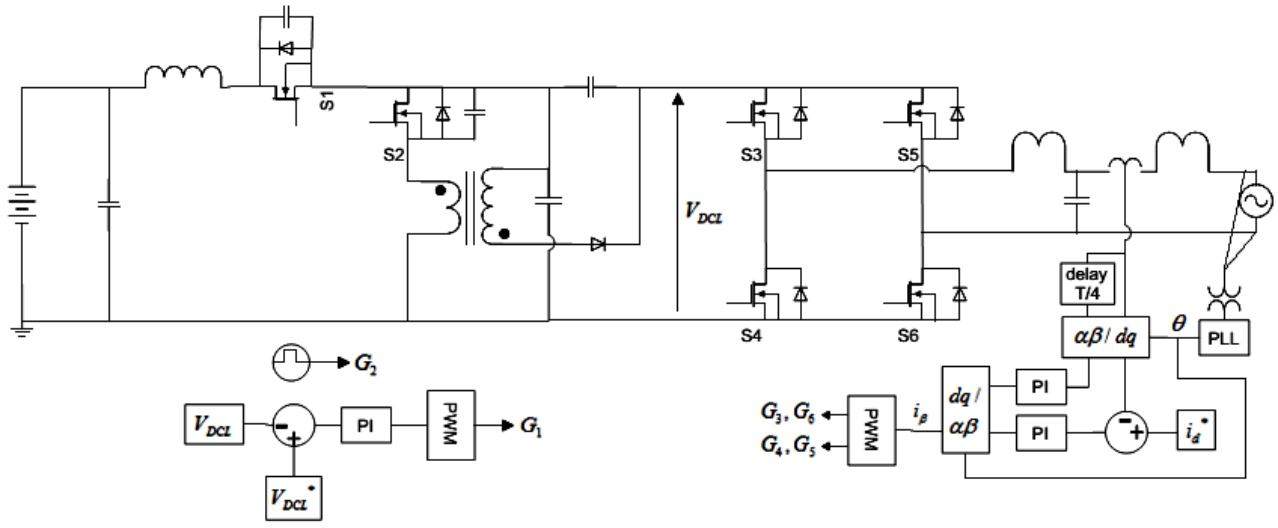

Fig. 4. Control strategy of the proposed soft switched grid connected inverter

$$i_{ds3,\max} = i_{ds4,\max} = i_{ds5,\max} = i_{ds6,\max} = \frac{\sqrt{2}P_{o,\max}}{V_{o,rms}} \quad (13)$$

$$v_{ds3,\max} = v_{ds4,\max} = v_{ds5,\max} = v_{ds6,\max} \approx V_{C1} + V_{C2} = \frac{V_{C1}}{1-D} \quad (14)$$

$$i_{ds1,\max} = \frac{P_{o,\max}}{V_{in}} \quad (15)$$

$$v_{ds1,\max} = V_{C1} + V_{C2} \quad (16)$$

The maximum current through power switch S_2 and the maximum voltage across it can be obtained from the following equations:

$$i_{ds2,\max} \approx I_{in} + i_{o,\max} + \frac{V_{C1} + V_{C2}(n-1/n)}{Z_o} = \frac{P_{o,\max}}{V_{in}} + \frac{\sqrt{2}P_{o,\max}}{V_{o,rms}} + \frac{V_{C1} + V_{C2}(n-1/n)}{Z_o} \quad (17)$$

$$v_{ds2,\max} \approx V_{C1} + V_{C2}(1+1/n) \quad (18)$$

where, n is the turn ratio of high frequency transformer and Z_0 is defined in equation (20). The resonant inductor maximum current $i_{Lin,max}$ is obtained through the following relation:

$$i_{Lin,\max} = i_{C1,\max} + i_{L1,\max} + \frac{V_{C2}(n-1)}{n\,Z_o} \quad (19)$$

In Equation (18), it is obvious that high values of Z_o will cause lower current flowing through power switch S_1, thus reducing the current stress of power switch S_1. Likewise, we have the following equation:

$$Z_o = \sqrt{L_{in}/C_{S1}} \quad (20)$$

Furthermore, we can write the following relation:

$$C_{S1} = L_{in}/Z_o^{\,2} \quad (21)$$

Therefore, in order to have a large value for Z_o, capacitor C_{S1} should have a relatively small value. Output filter inductor L_1 and capacitor C_3 are chosen such that to reduce the harmonics contents of the output voltage, which are a part of output LCL filter.

3. SIMULATION RESULTS

The drain-to-source current, gate-to-source voltage, and drain-to-source voltage for power switch S_2 are presented in Fig. 5. As this figure indicates, power switch S_1 is turned on and turned off with ZVS and ZCS, respectively. Similarly, the drain-to-source current, gate-to-source voltage, and drain-to-source voltage for power switch S_2 are depicted in Fig. 6. As shown in Fig. 6, power switch S_2 is turned on and turned off with ZVS and ZCS, respectively.

4. EXPERIMENTAL RESULTS

To illustrate the proper operation of the theoretical analysis and investigate whether it was accurately implemented in the present study, an experimental prototype of the proposed soft-switched grid-tied inverter was built. A photograph of the proposed converter is shown in Fig. 7. The real drain-to-source current, gate-to-source voltage, and drain-to-source voltage for power switch S_1 are demonstrated in Fig. 9. The ZVS turn-on condition for power switch S_1 is illustrated in Fig. 10. Moreover, the ZCS turn-off condition for power switch S_1 is depicted in Fig. 11. The real drain-to-source current, gate-to-source voltage, and drain-to-source voltage for power switch S_2 are shown in Fig. 12. The ZVS turn-on condition for power switch S_2 is illustrated in Fig. 13. In addition, the ZCS turn-off condition for power switch S_2 is depicted in Fig. 14. The real drain-to-source current, gate-to-source voltage, and drain-to-source voltage for power switch S_3 are presented in Fig. 15. The ZVS turn-on condition for power switch S_3 is illustrated in Fig. 16 and the ZCS turn-off condition for power switch S_3 is depicted in Fig. 17. Furthermore, the grid voltage, inverter output current, and inverter output voltage are shown in Fig. 18.

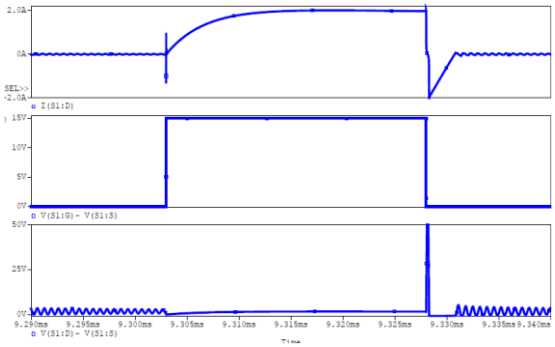

Fig. 5. Drain to source current (top), gate to source voltage (middle) and drain to source voltage (bottom) for power switch S_1

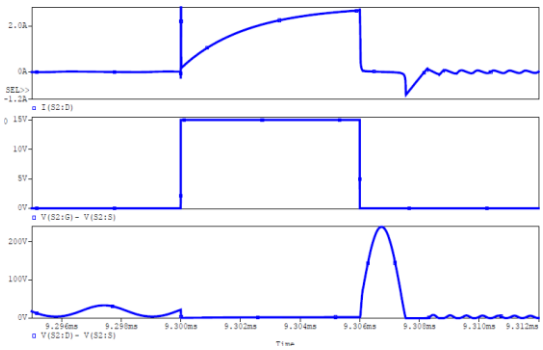

Fig. 6. Drain to source current (top), gate to source voltage (middle) and drain to source voltage (bottom) for power switch S_2

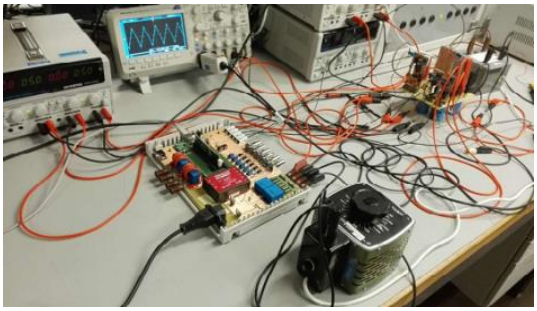

Fig. 7. A photograph of the proposed grid-tied inverter

Furthermore, grid voltage, grid-tied inverter output current, and grid-tied inverter output voltage are depicted in Fig. 19. The following components and characteristics have been used in the proposed soft-switched grid-tied inverter experimental prototype:

Input voltage: 150 VDC

Output voltage: $v_o(t) = 220\sqrt{2}\sin[2\pi(50)]t$

Output power: 1000 W maximum

Switching frequency: 20 kHz

HF transformer turns ratio: 2

Capacitor C1: 470 µF

DC-link capacitor C2: 470 µF

Input capacitor Cin: 470 µF

Resonant inductor Lin: 5 µH

Resonant capacitor CS1 and CS2: 2.2 nF

Switches S1, S2, S3, S4, S5, and S6: IRF840

Power diodes: 1N5408

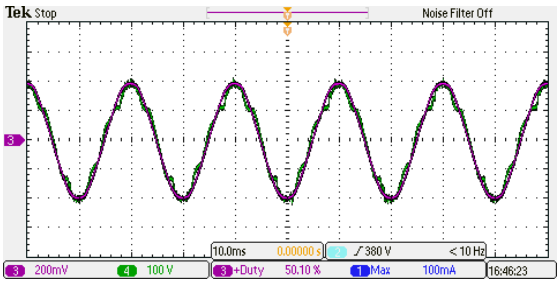

Fig. 8. Inverter output and grid voltages

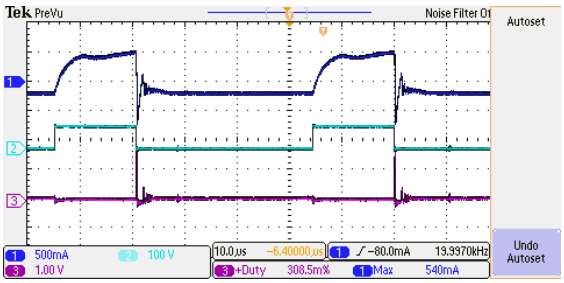

Fig. 9. Measured drain to source current (top), gate to source voltage (middle) and drain to source voltage (bottom) for power switch S_1

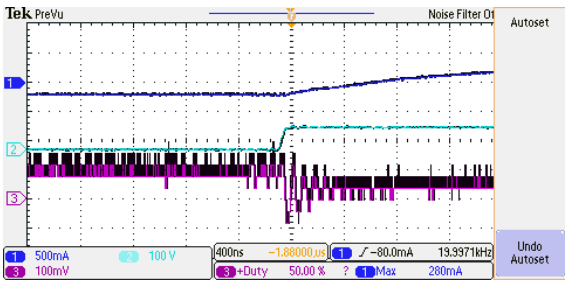

Fig. 10. Measured drain to source current (top), gate to source voltage (middle) and drain to source voltage (bottom) for power switch S_1

The efficiency diagram of the proposed soft-switched DC-DC converter, which was compared with that of the conventional DC-DC boost converter, active clamp push pull converter [35] and the system proposed in literature [27] is Illustrated in Fig. 20.

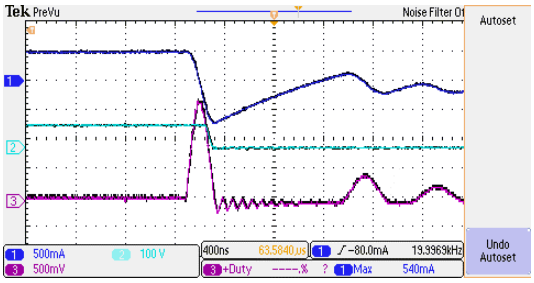

Fig. 11. Measured drain to source current (top), gate to source voltage (middle) and drain to source voltage (bottom) for power switch S_1

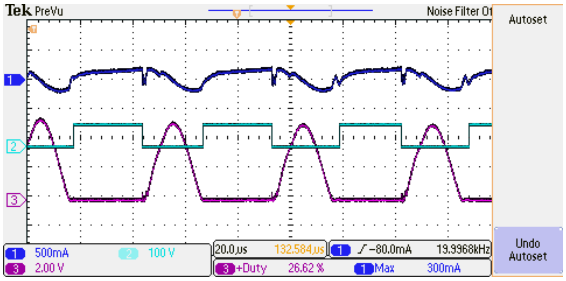

Fig. 12. Measured drain to source current (top), gate to source voltage (middle) and drain to source voltage (bottom) for power switch S_2

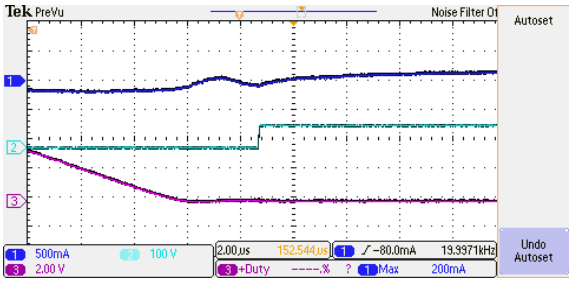

Fig. 13. Measured drain to source current (top), gate to source voltage (middle) and drain to source voltage (bottom) for power switch S_2

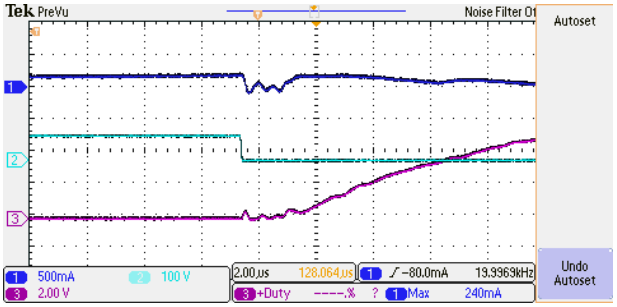

Fig. 14. Measured drain to source current (top), gate to source voltage (middle) and drain to source voltage (bottom) for power switch S_2

As depicted in this figure, the proposed soft-switched DC-DC converter reaches high power efficiency for almost 97.5% under the power between 800 W and 1000 W, being far superior to the hard-switching DC-DC boost converter and other existing topologies.

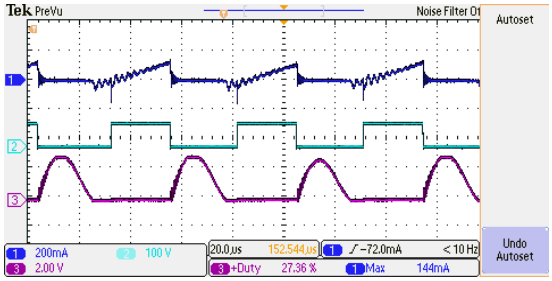

Fig. 15. Measured drain to source current (top), gate to source voltage (middle) and drain to source voltage (bottom) for power switch S_3

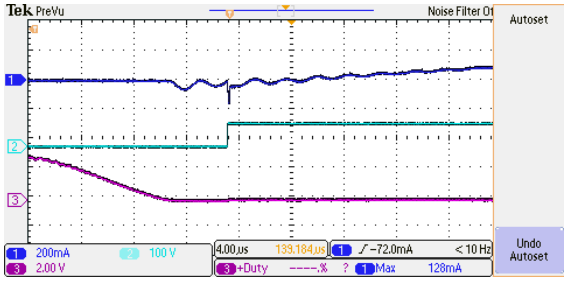

Fig. 16. Measured drain to source current (top), gate to source voltage (middle) and drain to source voltage (bottom) for power switch S

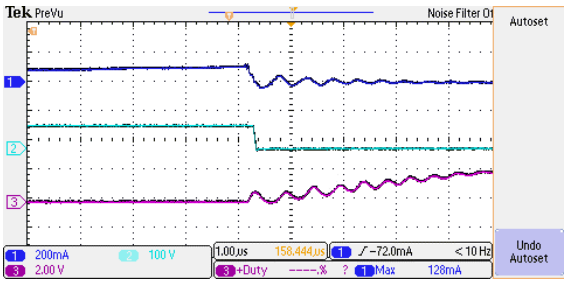

Fig. 17. Measured drain to source current (top), gate to source voltage (middle) and drain to source voltage (bottom) for power switch S_3

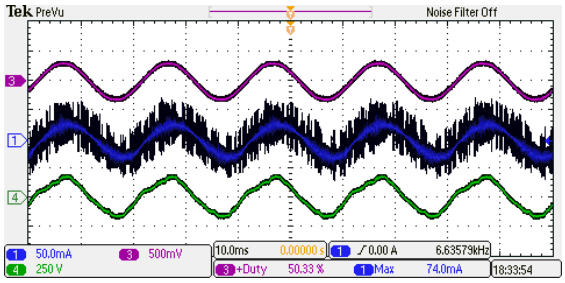

Fig. 18. Grid voltage (top), inverter output current (middle) and inverter output voltage (bottom)

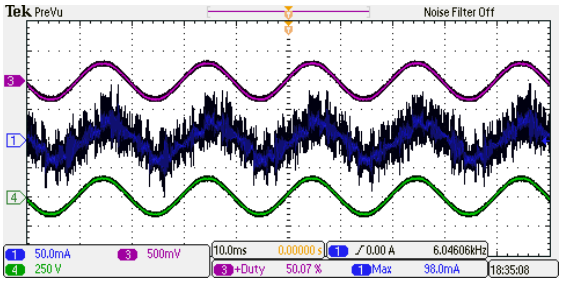

Fig. 19. Grid voltage (top), grid-tied inverter output current (middle) and grid-tied inverter output voltage (bottom)

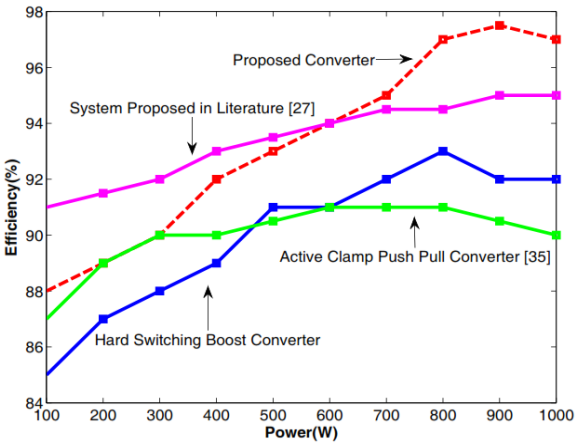

Fig. 20. Efficiency comparison of the proposed soft-switched DC-DC boost converter and existing converters

5. CONCLUSIONS

The soft-switched grid-tied inverter presented in this paper demonstrated a novel and highly efficient topology and control strategy because of using soft-switching techniques for commutation of power switches. Simulation results were prepared via ORCAD software in order to validate the proposed analysis and design. The experimental prototype verified the functionality and performance of the design and analysis. Furthermore, the experimental results indicated the accuracy of the analysis and high performance of the proposed topology and the applied control strategy.

References

[1] B. J. Pierquet, and D. J. Perreault, "A single phase photovoltaic inverter topology with a series-connected energy buffer", *IEEE Trans. Power Electron.*, vol.28, no.10, pp. 4603-4611, 2013.

[2] U. R. Prasanna, and A. K. Rathore, "Analysis, design and experimental results of a novel soft switching snubberless current-fed half-bridge front-end converter-based PV inverter", *IEEE Trans. Power Electron.*, vol. 28, no.7, pp. 3219-3230, 2013.

[3] T. D. Batzel, and K. Adams, "Variable timing control for ARCP voltage source inverters operating at low dc voltage", *Int. J. Mod. Eng.*, vol.13, no.2, pp. 41-50, 2013.

[4] Q.Li and P.Wolfs, "A current fed two-inductor boost converter with an integrated magnetic structure and passive lossless snubbers for photovoltaic module integrated converter applications," *IEEE Trans. Power Electron.*, vol. 22, no. 1, pp. 309-321, 2007.

[5] S. Jain and V. Agarwal, "An integrated hybrid power supply for distributed generation applications fed by nonconventional energy sources," *IEEE Trans. Energy Convers.*, vol. 23, no. 2, pp. 622-631, 2008.

[6] M. H. Todorovic, L. Palma, and P. Enjeti, "Design of a wide input range dc-dc converter with a robust power control scheme suitable for fuel cell power conversion," *IEEE Trans. Ind. Electron.*, vol. 55, no. 3, pp. 1247-1255, 2008.

[7] A. K. Rathore, A. K. S. Bhat, and R. Oruganti, "A

comparison of soft-switched dc-dc converters for fuel cell to utility interface application," *IEEE Trans. Ind. Appl.*, vol. 128, no. 4, pp. 450-458, 2008.

[8] IEEE Standard for Interconnecting Distributed Resources with Electric Power System, *IEEE stand. 1547*, 2003.

[9] G. Island, "Photovoltaics: design and installation manual", *Solar Energy Int., New Soc. Publishers*, p. 80, 2006.

[10] D. Ton, and W. Bower, Summary report on the doe high-tech inverter workshop, 2005.

[11] T. Esram, P. L. Chapman, "Comparison of photovoltaic array maximum power point tracking techniques," *IEEE Trans. Energy Convers.*, vol. 22, no. 2, pp. 439-449, 2007.

[12] M. Pakdel and S. Jalilzadeh, "A novel topology and control strategy for a soft-switched single-phase grid connected inverter," *J. Electr. Syst. Inf. Technol.*, vol. 3, no. 1, pp. 81-93, 2016.

[13] H. Keyhani, M. Johnson, and H. A. Toliyat. "A soft-switched highly reliable grid-tied inverter for PV applications," *Proc. Appl. Power Electron. Conf.*, 2014, pp. 1725-1732.

[14] Y. Fang, Z. H. Liu, and J. W. Zhang, "Design of resonant soft-switching grid-connected inverter," *Int. Appl. Mech. Mater.*, vol. 263, 2012, pp. 43-47.

[15] A, Damrong, S. Premrudeepreechacharn, and K. Higuchi, "An improved soft-switching single-phase inverter for small grid-connected PV-system," *Proc. Ind. Electron, 2008*, pp. 2125-2130.

[16] S. H. Park, G. R. Cha, Y. C. Jung, and C. Y. Won. "Design and application for PV generation system using a soft-switching boost converter with SARC," *IEEE Trans. Ind. Electron.*, vol. 57, no. 2, pp. 515-522, 2010.

[17] D. Y. Jung, Y. H. Ji, S. H. Park, Y. C. Jung, and C. Y. Won, "Interleaved soft-switching boost converter for photovoltaic power-generation system," *IEEE Trans. Power Electron.*, vol. 26, no. 4, pp. 1137-1145, 2011.

[18] H. L. Do, "A soft-switching DC/DC converter with high voltage gain," *IEEE Trans. Power Electron.*, vol. 25, no. 5, pp. 1193-1200, 2010.

[19] S. H. Park, S. R. Park, J. S. Yu, Y. C. Jung, and C. Y. Won. "Analysis and design of a soft-switching boost converter with an HI-bridge auxiliary resonant circuit*," IEEE Trans. Power Electron.*, vol. 25, no. 8, pp. 2142-2149, 2010.

[20] T. F. Wu, Y. D. Chang, C. H. Chang, and J. G. Yang. "Soft-switching boost converter with a flyback snubber for high power applications," *IEEE Trans. Power Electron.*, vol. 27, no. 3, pp. 1108-1119, 2012.

[21] W. Huang, X. Gao, S. Bassan, G. Moschopoulos, "Novel dual auxiliary circuits for ZVT-PWM converters," *Can. J. Electr. Comput. Eng.*, vol. 33, no. 3, pp. 153-160, 2008.

[22] H. Bodur, A. F. Bakan, "A New Zvt-Zct-Pwm DC-DC Converter," *IEEE Trans. Power Electron.*, vol. 3, no. 3, pp. 676-84, 2004.

[23] B. Akin, "An improved ZVT–ZCT PWM DC–DC boost converter with increased efficiency," *IEEE Trans. Power Electron.*, vol. 4, no. 4, pp. 1919-1926, 2014.

[24] C. D. Stein, H. L. Hey, "A true ZCZVT commutation cell for PWM converters," *Proc. Appl. Power Electron. Conf.*, Anaheim, CA, USA, 1998, vol. 2, pp. 1070-1076.

[25] N. Altintas, A. F. Bakan, I. Aksoy, "A novel zvt-zct-pwm boost converter," *IEEE Trans. Power Electron.*, vol. 29, no. 1, pp. 256-265, 2014.

[26] S. J. Kim, H. L. Do, "Soft-switching step-up converter with ripple-free output current," *IEEE Trans. Power Electron.*, vol. 31, no. 8, pp. 5618-5624, 2016.

[27] M. Das, V. Agarwal "Design and analysis of a high efficiency DC-DC converter with soft switching capability for renewable energy applications requiring high voltage gain," *IEEE Trans. Ind. Electron.*, vol. 63, no. 5, pp. 2936-44, 2016.

[28] R. N. Silva, F. L. Tofoli, P. P. Praca, D. de Souza Oliveira, L. H. Barreto, "Soft switching high voltage gain dc-dc interleaved boost converter," *IET Power Electron.*, vol. 8, no. 1, pp. 120-129, 2014.

[29] X. Lin, J. Xu, X. Zhou, G. Zhou, "Zero-voltage zero-current switching dc/dc converter with high step-up and high efficiency," *Electron. Lett.*, vol. 1, no. 14, pp. 1250-1252, 2016.

[30] D. Y. Jung, Y. H. Ji, S. H. Park, Y. C. Jung, C. Y. Won, "Interleaved soft-switching boost converter for photovoltaic power-generation system," *IEEE Trans. Power Electron.*, vol. 26, no. 4, pp. 1137-1145, 2014.

[31] S. Sathyan, H. Suryawanshi, B. Singh, C. Chakraborty, V. Verma, M. Ballal, "ZVS-ZCS high voltage gain integrated boost converter for DC microgrid," *IEEE Trans. Ind. Electron.*, vol. 3, no. 3, pp. 0278-0046, 2016.

[32] Q. Zhao, F. C. Lee, "High-efficiency, high step-up DC-DC converters," *IEEE Trans. Power Electron.*, vol. 18, no. 1, pp. 65-73, 2003.

[33] K. C. Tseng, T. J. Liang, "Novel high-efficiency step-up converter," *IEE Proc. Electr. Power Appl.*, vol. 151, no.2, pp. 182-190, 2004.

[34] S. Dwari, L. Parsa, "An efficient high-step-up interleaved DC–DC converter with a common active clamp," *IEEE Trans. Power Electron.*, vol. 26, no. 1, pp. 66-78, 2011.

[35] T. F. Wu, Y. S. Lai, J. C. Hung, Y. M. Chen "Boost converter with coupled inductors and buck-boost type of active clamp," *Proc. IEEE Power Electron. Spec. Conf., 2005*, pp. 399-405.